Optical Thermometry of an Electron Reservoir Coupled to a Single Quantum Dot in the Millikelvin Range

F. Seilmeier, M. Hauck, E. Schubert, G. J. Schinner, S. E. Beavan,* and A. Högele†

Fakultät für Physik and Center for NanoScience (CeNS), Ludwig-Maximilians-Universität München, Geschwister-Scholl-Platz 1, 80539 München, Germany

(Received 9 May 2014; published 1 August 2014)

We show how resonant laser spectroscopy of the trion optical transitions in a self-assembled quantum dot can be used to determine the temperature of a nearby electron reservoir. At finite magnetic field, the spin-state occupation of the Zeeman-split quantum-dot electron ground states is governed by thermalization with the electron reservoir via cotunneling. With resonant spectroscopy of the corresponding excited trion states, we map out the spin occupation as a function of magnetic field to establish optical thermometry for the electron reservoir. We demonstrate the implementation of the technique in the subkelvin temperature range where it is most sensitive and where the electron temperature is not necessarily given by the cryostat base temperature.

DOI: 10.1103/PhysRevApplied.2.024002

I. INTRODUCTION

Self-assembled semiconductor quantum dots (QDs) represent promising building blocks for quantum-information processing [1] and, more recently, have emerged as an intriguing model system for optical studies of the quantum-impurity problem—the interaction of a localized electron with the continuum of states in a fermionic reservoir [2]. In the regime of strong tunnel coupling of a resident QD electron to the nearby Fermi sea and sufficiently low temperatures, signatures of many-body phenomena are observable in emission [3] or absorption with power-law tails characteristic of the Fermi-edge singularity [4] and the Kondo effect [5] in resonant spectra of neutral and singly charged QDs. In addition to resonant laser spectroscopy of charge-tunable QDs [6] and the control of their exchange coupling to the Fermi reservoir enabled by the gate voltage in QD field-effect devices [7], related experiments crucially require cryogenic temperatures deep in the subkelvin regime [4,5].

While the temperature of the electron reservoir is a key parameter in exploiting many-body phenomena, it is not necessarily the same as that of the cryogenic bath and is difficult to access directly. In this article, we present a spectroscopic method to determine the electron-bath temperature. Our technique exploits the sensitivity of spin-selective optical absorption in singly charged QDs [8–10] to temperature. A measurement of the effective QD electron spin temperature can be directly related to the spin-bath temperature of the Fermi reservoir [11–13]. Although the QD-bath temperature relationship is complicated by optical spin pumping (OSP), in the limit of strong exchange coupling between the QD spin and the Fermi bath via cotunneling, the OSP is negligible, and the QD spin-state occupation is entirely governed by the thermal distribution of the electrons in the Fermi sea. In either case (with or without OSP), the QD electron spin polarization measured as a function of an external magnetic field provides a direct measure of the electron-bath temperature.

II. EXPERIMENTAL METHODS

In our experiment, we use self-assembled InGaAs quantum dots grown by molecular beam epitaxy [14] with intermediate annealing [15]. The QDs are embedded inside a field-effect device [16] where a 25-nm-thick GaAs tunneling barrier separates the QDs from a heavily-n^+-doped GaAs layer that forms the Fermi reservoir. The QD layer is capped subsequently by 10-nm GaAs, an AlGaAs/GaAs superlattice of 252 nm thickness, and 14 nm of GaAs. A semitransparent NiCr layer of 5 nm is evaporated on the surface to form the top electrode. A gate voltage applied to the top electrode tunes the QD energy levels relative to the Fermi level pinned in the back reservoir to control the QD charge occupation [17] and the exciton emission energy through the quantum-confined Stark effect [18]. Moreover, the gate voltage also varies the coupling between the QD electron spin and the Fermi reservoir (given by the cotunneling rate) by orders of magnitude [7].

The sample is mounted inside a ^{3}He refrigerator with a nominal minimum base temperature of $T_{\mathrm{base}} = 250$ mK [Fig. 1(a)]. The temperature is adjusted from 250 mK to 4.0 K by heating or pumping via the sorption pump on the ^{3}He pot. Optical access to the sample is provided by a fiber-based confocal microscope system with a spot size of approximately 1 μm [19], addressing sufficiently few dots for single-QD spectroscopy. We use the differential

*sarah@beavan.com.au
†alexander.hoegele@lmu.de

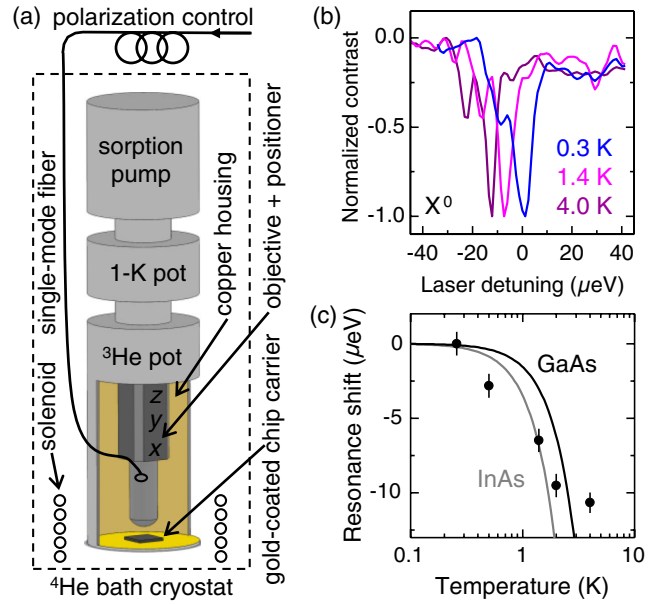

FIG. 1. (a) Experimental setup. The cryogenic system consists of a ^{3}He insert in a ^{4}He bath cryostat and provides a minimum base temperature of 250 mK. The solenoid is used to apply magnetic fields up to 10 T along the vertical axis of the cryostat. The quantum-dot sample is mounted on a gold-coated chip carrier in thermal contact with the ^{3}He pot. Optical access to individual quantum dots is enabled with a fiber-based micro-objective mounted on an *xyz* nanopositioner. (b) Differential transmission spectra of the neutral exciton (X^0) transition at cryostat base temperatures $T_{\text{base}} = 0.3$, 1.4, and 4.0 K show a resonance redshift with increasing temperature. (c) The X^0 resonance shift as a function of T_{base}. The gray and black lines represent the temperature shift expected in bulk InAs and GaAs, respectively.

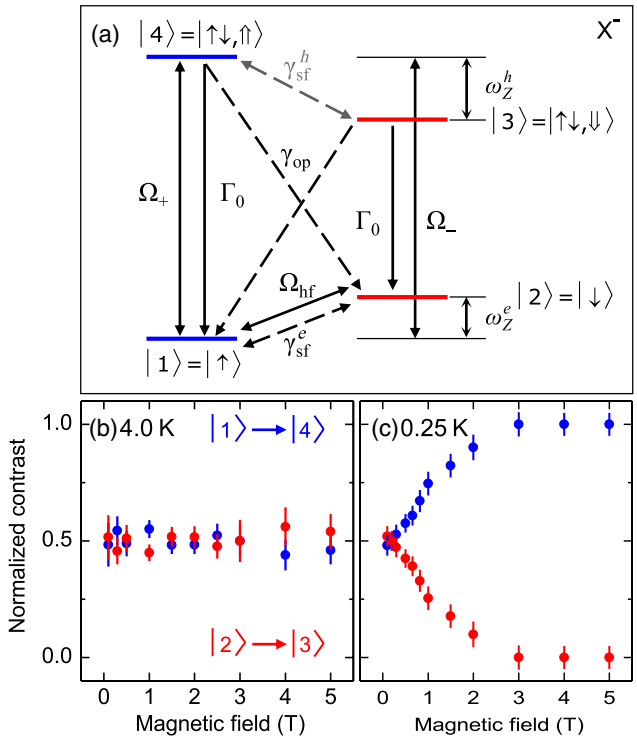

FIG. 2. (a) The four-level system associated with the X^- resonance in a charged QD, with a magnetic field applied in Faraday configuration. There are two dipole-allowed optical transitions associated with the upper $|1\rangle \leftrightarrow |4\rangle$ (blue transition) and lower $|2\rangle \leftrightarrow |3\rangle$ (red transition) Zeeman branches. The description of rates and Zeeman splittings is given in the text. (b),(c) Normalized contrast for both the red and blue transitions measured as a function of magnetic field with $T_{\text{base}} = 4.0$ K and 250 mK, respectively. At large magnetic fields and a sufficiently low temperature, the spin population accumulates in the spin-up ground state.

transmission method to address the neutral exciton (X^0) and trion (X^-) optical transitions in a single QD with resonant laser spectroscopy [6].

III. RESULTS

The evolution of the X^0 resonance with the temperature is shown in Figs. 1(b) and 1(c). Both fine-structure resonances of the neutral exciton exhibit a redshift with increasing temperature [data points in Fig. 1(b)] consistent with a decrease of the band-gap energy in semiconductors described by the Varshni relation [20] [solid lines for bulk InAs and GaAs in Fig. 1(b)]. The discrepancy between the measured resonance shift and the expected bulk values is not surprising given the uncertainty in both the material composition and the strain distribution inherent to self-assembled QDs. It also highlights the fact that a measurement of the resonance shift alone does not qualify as a reliable method for quantitative thermometry.

Instead, we exploit the temperature dependence of the spin-resolved trion optical transitions in finite magnetic field [8,9] to determine the electron-bath temperature. The level diagram of the X^- in the presence of an optical drive at finite magnetic field applied in Faraday geometry is shown in Fig. 2(a). The lower electron states with spin $\pm\frac{1}{2}$ (denoted as $|\uparrow\rangle = |1\rangle$ and $|\downarrow\rangle = |2\rangle$ and split by the electron Zeeman energy $\hbar\omega^e_Z = g_e\mu_B B$) couple to the trion states with two spin-singlet electrons and one heavy hole with spin $\pm\frac{3}{2}$ (denoted as $|\uparrow\downarrow\Uparrow\rangle = |4\rangle$ and $|\uparrow\downarrow\Downarrow\rangle = |3\rangle$ and separated by the hole Zeeman energy $\hbar\omega^h_Z = g_h\mu_B B$). The dipole-allowed transitions between the blue ($|1\rangle$-$|4\rangle$) and red ($|2\rangle$-$|3\rangle$) Zeeman branches can be selectively addressed by σ^+ and σ^- circularly polarized laser fields with respective Rabi frequencies Ω_+ and Ω_-.

For strongly confining QDs, the overlap between electron and hole wave functions, which determines the radiative decay rate Γ_0, is insensitive to magnetic field for realistic experimental field strengths, and, thus, Γ_0 can be treated as equivalent for both dipole-allowed transitions [21]. It also provides an upper bound on the dipole-forbidden diagonal transition rates $\gamma_{\text{op}} = \eta\Gamma_0$ that become weakly allowed by heavy-hole light-hole admixing with

$\eta \ll 1$ and contribute to OSP [11]. Although there is a temperature dependence in the incoherent hole spin-flip rate γ_{SF}^{h} [10,22,23], this effect is rendered negligible by the much faster optical decay channel, i.e., $\gamma_{\mathrm{op}} \gg \gamma_{\mathrm{SF}}^{h}$. Another temperature-insensitive parameter is the coherent coupling of the electron spin states mediated by the hyperfine interaction with a "frozen" nuclear spin environment. This leads to an effective coupling $\hbar\Omega_{\mathrm{hf}} \sim 1\ \mu\mathrm{eV}$ [11,24,25], while the analogous coherent coupling of the excited states is negligible due to much weaker hole hyperfine interaction [26,27]. Finally, since both the hyperfine-mediated and the spin-orbit-induced spin-flip processes are negligible in our experiment as compared to the spin-exchange rate with the Fermi reservoir via cotunneling (at a rate γ_{ct}), our inspection of the optically driven four-level system arrives at the conclusion that the only sensitivity to temperature stems from $\gamma_{\mathrm{SF}}^{e} = \gamma_{\mathrm{ct}}$. Importantly, the asymmetry between the ground-state occupations in the absence of OSP has an exponential dependence on the temperature $\gamma_{12} = \gamma_{21}\exp(-\omega_Z^e/k_BT)$. This fact is exploited in the following to determine the electron-bath temperature T_e with trion laser spectroscopy.

Experimentally, it is convenient to use linear polarization to address both trion transitions with one laser field scanned in frequency, and we choose $\Omega_+ = \Omega_- \simeq \Gamma_0$ to drive the transition close to saturation where the signal-to-noise ratio of the differential transmission contrast α is optimal [28]. Figures 2(b) and 2(c) summarize the results we obtain for the spin-resolved trion branches at different magnetic fields and temperatures. For finite magnetic fields, the two optical transitions are well resolved, and the peak amplitudes are used to calculate the normalized transmission contrast as $\alpha_{\mathrm{blue,red}}/(\alpha_{\mathrm{blue}} + \alpha_{\mathrm{red}})$ for the blue and red transitions accordingly.

The normalized contrasts in Figs. 2(b) and 2(c) correspond to nominal base temperatures of 4.0 K and 250 mK, respectively. While there is no significant evolution of the normalized contrast with magnetic field at 4.0 K, the relative strength of the blue transition grows at the expense of the red transition for the lowest temperature of our ^{3}He system. In this case, the normalized contrasts saturate for magnetic fields above 3 T, implying a negligible population of the state $|\downarrow\rangle$ and a spin accumulation in the $|\uparrow\rangle$ state. This asymptotic limit is expected for a thermal spin distribution in a singly charged QD governed by fast cotunneling processes [8]. At moderate magnetic fields, however, the spin-state population is modified by optical spin pumping [9] whenever $\gamma_{\mathrm{ct}} \simeq \gamma_{\mathrm{op}}$. In our sample with a nominal separation of 25 nm between the electron reservoir and the QD layer, we estimate the tunnel coupling γ_t [see Fig. 4(b)] in the range between 10 and 50 μeV for strongly confining QDs with emission around 1.3 eV. In the center of the trion stability plateau, the working point in our experiments, this implies a competition between effective thermal and optical spin-pumping rates at deep subkelvin temperatures, necessitating a full four-level system analysis.

IV. MODELING AND DISCUSSION

The four-level system is modeled using a Lindblad master equation similar to Ref. [10]. The Hamiltonian contains the coherent dynamics due to both optical fields Ω_+ and Ω_- with $\Omega_\pm = 2.5 \times \Gamma_0$, and the hyperfine term $\hbar\Omega_{\mathrm{hf}} = 1.3\ \mu\mathrm{eV}$. The incident laser field also drives the weakly allowed off-diagonal transitions with Rabi frequencies of $\eta\Omega_\pm$, where we take $\eta \approx 4 \times 10^{-4}$ [11]. The incoherent transition rates $\hbar\Gamma_0 = 1\ \mu\mathrm{eV}$, $\gamma_{\mathrm{op}} = \eta\Gamma_0$, $\gamma_{21} = \gamma_{\mathrm{ct}}$, and γ_{12} as defined above are included in the usual Lindblad superoperator formalism. The value of the cotunneling rate at the minimum base temperature of 250 mK is estimated as $\hbar\gamma_{\mathrm{ct}} \approx 5 \times 10^{-4}\ \mu\mathrm{eV}$ [7]. An additional term is included to account for the broadening of the optical resonance that is caused by environmental charge and spin fluctuations [6,29]; in our experiments, the observed resonance width is $\hbar\Gamma \approx 6\ \mu\mathrm{eV}$ [Fig. 1(b)]. We include the effect as pure dephasing of the excited states with a rate of $\Gamma_d/2 = 2.5\ \mu\mathrm{eV}$ that contributes to the experimental linewidth as $\Gamma = \Gamma_0 + \Gamma_d$. The electron and hole g factors are taken as $g_e = 0.69$ and $g_h = 0.81$ [12]. The steady-state solutions for the density matrix are found numerically [30] for both cases when the red and blue transitions are driven resonantly. The normalized absorption contrast is calculated using the relevant coherence terms of the density matrix.

The model is used to fit the data recorded at $T_{\mathrm{base}} = 250$ mK with the temperature as the only free parameter. The optimized fit gives a value of $T_e = 400 \pm 50$ mK. The solution of the four-level model is shown in Fig. 3(a), along with the result expected from a thermal population distribution between the two ground states. As expected for

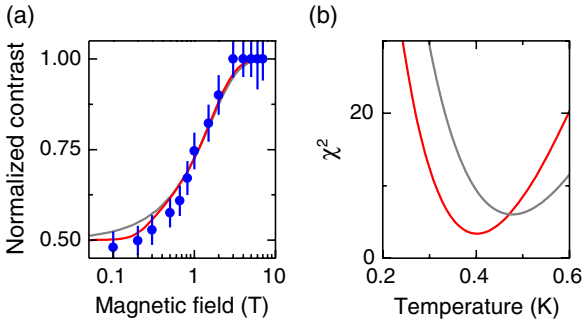

FIG. 3. (a) Normalized contrast measured at $T_{\mathrm{base}} = 250$ mK, along with the temperature-fit results using the full four-level model described in the text (red line, $T_e = 400$ K) and the two-level thermal model (gray line, $T_e = 480$ K). (b) The mean-squared "distance" between the data and the model predictions for the normalized contrast indicates a better fit by the four-level model (red line) as compared to the two-level thermal distribution (gray line).

this low value of γ_{ct} in our sample in the subkelvin regime, there is evidence of optically induced spin pumping at low magnetic field values (< 500 mT), where the normalized contrasts remain closer to 0.5 (i.e., equal population in both states $|1\rangle$ and $|2\rangle$) than would be expected in a purely thermodynamic equilibrium. The four-level model qualitatively captures this spin-pumping trend and, therefore, provides a better fit as compared to the two-level model [see Fig. 3(b)]. Despite large uncertainties in many of the input parameters to the four-level model, most of which are not measured specifically for this dot, the temperature can be determined with an accuracy of 12%. The temperature returned by the fit changes by less than 10% with variations in the values of η and Ω_{hf} by a factor of 2 or an order of magnitude change in γ_{ct}. The model is most sensitive to the values of Γ_0, $\Omega_{\pm}$, and $g_{e,h}$. In particular, the estimated $\pm 10\%$ uncertainty margin for the $g_{e,h}$ values is the largest contribution to the temperature uncertainty. Therefore, the temperature can be determined much more precisely by measuring the g factors for this dot using two-color spectroscopy [12].

For a general application of this thermometry method in alternate QD systems, it is desirable to eliminate this OSP signature and recover a simple two-level thermal system. We suggest two straightforward alterations that will allow for this simplification. First, the effectiveness of optically induced spin pumping can be reduced by pumping with circularly rather than linearly polarized light, such that only one of the optical transitions is driven efficiently at small magnetic fields. Second, the relaxation rate γ_{ct} can be increased relative to the optical spin-pumping channel given by rates $\Omega_{\pm}$ and γ_{op}. The value of γ_{ct} can be controllably tuned across a few orders of magnitude by varying the gate voltage and can be further altered for different samples by tailoring the tunnel-barrier energy itself. Figure 4(a) shows how the cotunneling rate varies with gate voltage for a number of different tunnel-barrier energies and also for different temperatures [7]. It will, in most cases, be possible to increase γ_{ct} sufficiently by tuning the gate voltage [shaded regions in Fig. 4(a)] and move into an elegantly simple regime where the normalized contrast directly reflects a thermal distribution in a two-level system.

Another mechanism through which the system dynamics will significantly deviate from that of a two-level thermal distribution can arise due to the dynamic interaction between the electron spin and the 10^5 nuclear spins in the QD [31]. The effect known as dragging (antidragging) occurs when the electron spin causes the nuclear spins to align in such a way as to Zeeman shift the transition into (out of) resonance with the incident light [32,33]. This effect is particularly pronounced at high magnetic fields, long integration times, and when the step size of the laser frequency sweep is small. In the current experiment, the dragging effects are minimized by choosing a large laser step size. An alternative method to eliminate nuclear spin magnetization is to actively depolarize the nuclear spin ensemble [34].

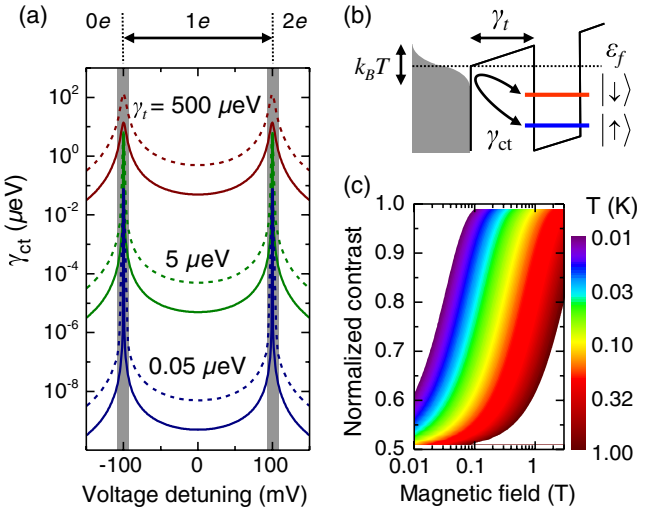

FIG. 4. (a) Optimal working regions for optical thermometry of the electron reservoir at the edges of the charge stability plateau are shaded gray. The cotunneling rate γ_{ct} is plotted as a function of gate voltage detuning from the plateau center for 400 and 40 mK as dashed and solid lines according to Ref. [7]. (b) At the edges, the cotunneling rate between the quantum-dot electron states and the Fermi edge ε_F thermally broadened by k_BT is maximum for a sample-specific tunnel coupling γ_t (500, 5, and 0.05 μeV roughly correspond to tunneling barriers of 15, 25, and 35 nm). Tuning to the maximum γ_{ct} simplifies the system dynamics to an effective thermal two-level system, and a single measurement of the normalized contrast at a particular applied magnetic field should suffice to determine the temperature of the electron reservoir using the color map shown in (c).

If the experimental conditions are chosen such that the two-level approximation is valid, then the electron reservoir temperature T_e can be read out with a single normalized-contrast measurement using the color map shown in Fig. 4(c). To quantify the precision of this method in determining the temperature, we use the best-case signal-to-noise ratios achievable with either differential transmission measurements (6×10^3 using a GaAs solid immersion lens [35]) or resonance fluorescence (10^5 [29]). This results in a temperature measurement with uncertainty as low as 0.004% using resonance fluorescence or 0.06% with differential transmission spectroscopy. Therefore, this method could potentially measure mK temperatures with sub-μK precision.

V. CONCLUSION

In conclusion, we develop and demonstrate a novel technique to determine the temperature of an electron spin bath. This is achieved by optically driving a QD tunnel coupled to the electron spin bath and monitoring its spin polarization as a function of magnetic field. At mK

temperatures, the actual temperature of the electron reservoir can deviate significantly from the nominal base temperature of the cryostat, as is the case here where the temperature is determined as 400 ± 50 mK at a cryostat base temperature of 250 mK. By maximizing the cotunneling rate γ_{ct} via the gate voltage, the four-level system description simplifies to a two-level thermal system, allowing for a straightforward and simple method of electron-bath thermometry. The sensitivity of this method is optimal at low temperatures ($T < 1$ K). The parameter range of low temperatures and large cotunneling rates coincides with the regime of interest for exploring the many-body interactions between a QD and an electron bath, where the reservoir temperature is an important parameter. Thus, the optical thermometry technique will be a particularly useful tool in future investigations of many-body phenomena in self-assembled QD systems.

We would like to acknowledge the work by Haupt *et al.* that appeared recently [36].

ACKNOWLEDGMENTS

We acknowledge A. Badolato and P. M. Petroff for growing the sample heterostructure used in this work and M. Kroner for useful discussions. This research is funded by the Deutsche Forschungsgemeinschaft (SFB 631 and the German Excellence Initiative via the Nanosystems Initiative Munich, NIM) with support from the Center for NanoScience (CeNS) and LMUexcellent.

[1] A. Imamoğlu, H. Schmidt, G. Woods, and M. Deutsch, Strongly interacting photons in a nonlinear cavity, Phys. Rev. Lett. **79**, 1467 (1997).

[2] H. E. Türeci, M. Hanl, M. Claassen, A. Weichselbaum, T. Hecht, B. Braunecker, A. O. Govorov, L. Glazman, A. Imamoğlu, and J. von Delft, Many-body dynamics of exciton creation in a quantum dot by optical absorption: A quantum quench towards Kondo correlations, Phys. Rev. Lett. **106**, 107402 (2011).

[3] N. A. J. M. Kleemans, J. van Bree, A. O. Govorov, J. G. Keizer, G. J. Hamhuis, R. Nötzel, A. Y. Silov, and P. M. Koenraad, Many-body exciton states in self-assembled quantum dots coupled to a Fermi sea, Nat. Phys. **6**, 534 (2010).

[4] F. Haupt, S. Smolka, M. Hanl, W. Wüster, J. Miguel-Sanchez, A. Weichselbaum, J. von Delft, and A. Imamoğlu, Nonequilibrium dynamics in an optical transition from a neutral quantum dot to a correlated many-body state, Phys. Rev. B **88**, 161304 (2013).

[5] C. Latta, F. Haupt, M. Hanl, A. Weichselbaum, M. Claassen, W. Wuester, P. Fallahi, S. Faelt, L. Glazman, J. von Delft, H. E. Türeci, and A. Imamoğlu, Quantum quench of Kondo correlations in optical absorption, Nature (London) **474**, 627 (2011).

[6] A. Högele, S. Seidl, M. Kroner, K. Karrai, R. J. Warburton, B. D. Gerardot, and P. M. Petroff, Voltage-controlled optics of a quantum dot, Phys. Rev. Lett. **93**, 217401 (2004).

[7] J. M. Smith, P. A. Dalgarno, R. J. Warburton, A. O. Govorov, K. Karrai, B. D. Gerardot, and P. M. Petroff, Voltage control of the spin dynamics of an exciton in a semiconductor quantum dot, Phys. Rev. Lett. **94**, 197402 (2005).

[8] A. Högele, M. Kroner, S. Seidl, K. Karrai, M. Atatüre, J. Dreiser, A. Imamoğlu, R. J. Warburton, A. Badolato, B. D. Gerardot, and P. M. Petroff, Spin-selective optical absorption of singly charged excitons in a quantum dot, Appl. Phys. Lett. **86**, 221905 (2005).

[9] M. Atatüre, J. Dreiser, A. Badolato, A. Högele, K. Karrai, and A. Imamoğlu, Quantum-dot spin-state preparation with near-unity fidelity, Science **312**, 551 (2006).

[10] B. D. Gerardot, D. Brunner, P. A. Dalgarno, P. Ohberg, S. Seidl, M. Kroner, K. Karrai, N. G. Stoltz, P. M. Petroff, and R. J. Warburton, Optical pumping of a single hole spin in a quantum dot, Nature (London) **451**, 441 (2008).

[11] J. Dreiser, M. Atatüre, C. Galland, T. Müller, A. Badolato, and A. Imamoğlu, Optical investigations of quantum dot spin dynamics as a function of external electric and magnetic fields, Phys. Rev. B **77**, 075317 (2008).

[12] M. Kroner, K. M. Weiss, B. Biedermann, S. Seidl, A. W. Holleitner, A. Badolato, P. M. Petroff, P. Öhberg, R. J. Warburton, and K. Karrai, Resonant two-color high-resolution spectroscopy of a negatively charged exciton in a self-assembled quantum dot, Phys. Rev. B **78**, 075429 (2008).

[13] C. Latta, A. Srivastava, and A. Imamoğlu, Hyperfine interaction-dominated dynamics of nuclear spins in self-assembled InGaAs quantum dots, Phys. Rev. Lett. **107**, 167401 (2011).

[14] D. Leonard, M. Krishnamurthy, C. M. Reaves, S. P. Denbaars, and P. M. Petroff, Direct formation of quantum-sized dots from uniform coherent islands of InGaAs on GaAs surfaces, Appl. Phys. Lett. **63**, 3203 (1993).

[15] J. M. Garcia, G. Medeiros-Ribeiro, K. Schmidt, T. Ngo, J. L. Feng, A. Lorke, J. P. Kotthaus, and P. M. Petroff, Intermixing and shape changes during the formation of InAs self-assembled quantum dots, Appl. Phys. Lett. **71**, 2014 (1997).

[16] H. Drexler, D. Leonard, W. Hansen, J. P. Kotthaus, and P. M. Petroff, Spectroscopy of quantum levels in charge-tunable InGaAs quantum dots, Phys. Rev. Lett. **73**, 2252 (1994).

[17] R. J. Warburton, C. Schaflein, D. Haft, F. Bickel, A. Lorke, K. Karrai, J. M. Garcia, W. Schoenfeld, and P. M. Petroff, Optical emission from a charge-tunable quantum ring, Nature (London) **405**, 926 (2000).

[18] R. J. Warburton, C. Schulhauser, D. Haft, C. Schäflein, K. Karrai, J. M. Garcia, W. Schoenfeld, and P. M. Petroff, Giant permanent dipole moments of excitons in semiconductor nanostructures, Phys. Rev. B **65**, 113303 (2002).

[19] A. Högele, S. Seidl, M. Kroner, K. Karrai, C. Schulhauser, O. Sqalli, J. Scrimgeour, and R. J. Warburton, Fiber-based confocal microscope for cryogenic spectroscopy, Rev. Sci. Instrum. **79**, 023709 (2008).

[20] Y. P. Varshni, Temperature dependence of the energy gap in semiconductors, Physica (Utrecht) **34**, 149 (1967).

[21] R. J. Warburton, B. T. Miller, C. S. Dürr, C. Bödefeld, K. Karrai, J. P. Kotthaus, G. Medeiros-Ribeiro, P. M. Petroff, and S. Huant, Coulomb interactions in small charge-tunable quantum dots: A simple model, Phys. Rev. B **58**, 16221 (1998).

[22] D. Brunner, B. D. Gerardot, P. A. Dalgarno, G. Wüst, K. Karrai, N. G. Stoltz, P. M. Petroff, and R. J. Warburton, A coherent single-hole spin in a semiconductor, Science **325**, 70 (2009).

[23] J. Houel, A. V. Kuhlmann, L. Greuter, F. Xue, M. Poggio, B. D. Gerardot, P. A. Dalgarno, A. Badolato, P. M. Petroff, A. Ludwig, D. Reuter, A. D. Wieck, and R. J. Warburton, Probing single-charge fluctuations at a GaAs/AlAs interface using laser spectroscopy on a nearby InGaAs quantum dot, Phys. Rev. Lett. **108**, 107401 (2012).

[24] A. S. Bracker, E. A. Stinaff, D. Gammon, M. E. Ware, J. G. Tischler, A. Shabaev, A. L. Efros, D. Park, D. Gershoni, V. L. Korenev, and I. A. Merkulov, Optical pumping of the electronic and nuclear spin of single charge-tunable quantum dots, Phys. Rev. Lett. **94**, 047402 (2005).

[25] P. -F. Braun, X. Marie, L. Lombez, B. Urbaszek, T. Amand, P. Renucci, V. K. Kalevich, K. V. Kavokin, O. Krebs, P. Voisin, and Y. Masumoto, Direct observation of the electron spin relaxation induced by nuclei in quantum dots, Phys. Rev. Lett. **94**, 116601 (2005).

[26] P. Fallahi, S. T. Yilmaz, and A. Imamoğlu, Measurement of a heavy-hole hyperfine interaction in InGaAs quantum dots using resonance fluorescence, Phys. Rev. Lett. **105**, 257402 (2010).

[27] E. A. Chekhovich, M. N. Makhonin, K. V. Kavokin, A. B. Krysa, M. S. Skolnick, and A. I. Tartakovskii, Pumping of nuclear spins by optical excitation of spin-forbidden transitions in a quantum dot, Phys. Rev. Lett. **104**, 066804 (2010).

[28] B. D. Gerardot, S. Seidl, P. A. Dalgarno, R. J. Warburton, M. Kroner, K. Karrai, A. Badolato, and P. M. Petroff, Contrast in transmission spectroscopy of a single quantum dot, Appl. Phys. Lett. **90**, 221106 (2007).

[29] A. V. Kuhlmann, J. Houel, A. Ludwig, L. Greuter, D. Reuter, A. D. Wieck, M. Poggio, and R. J. Warburton, Charge noise and spin noise in a semiconductor quantum device, Nat. Phys. **9**, 570 (2013).

[30] J. Johansson, P. Nation, and F. Nori, QuTiP 2: A Python framework for the dynamics of open quantum systems, Comput. Phys. Commun. **184**, 1234 (2013).

[31] B. Urbaszek, X. Marie, T. Amand, O. Krebs, P. Voisin, P. Maletinsky, A. Högele, and A. Imamoğlu, Nuclear spin physics in quantum dots: An optical investigation, Rev. Mod. Phys. **85**, 79 (2013).

[32] A. Högele, M. Kroner, C. Latta, M. Claassen, I. Carusotto, C. Bulutay, and A. Imamoğlu, Dynamic nuclear spin polarization in the resonant laser excitation of an InGaAs quantum dot, Phys. Rev. Lett. **108**, 197403 (2012).

[33] W. Yang and L. J. Sham, Collective nuclear stabilization in single quantum dots by noncollinear hyperfine interaction, Phys. Rev. B **85**, 235319 (2012).

[34] E. A. Chekhovich, K. V. Kavokin, J. Puebla, A. B. Krysa, M. Hopkinson, A. D. Andreev, A. M. Sanchez, R. Beanland, M. S. Skolnick, and A. I. Tartakovskii, Structural analysis of strained quantum dots using nuclear magnetic resonance, Nat. Nanotechnol. **7**, 646 (2012).

[35] A. N. Vamivakas, M. Atatüre, and J. Dreiser, Strong extinction of a far-field laser beam by a single quantum dot, Nano Lett. **7**, 2892 (2007).

[36] F. Haupt, A. Imamoglu, M. Kroner, preceding paper, Single quantum dot as an optical thermometer for millikelvin temperatures, Phys. Rev. Applied **2**, 024001 (2014).